Nat Hazards
DOI 10.1007/s11069-015-1700-3

ORIGINAL PAPER

An integrated assessment of soil erosion dynamics with special emphasis on gully erosion in the Mazayjan basin, southwestern Iran

Reza Zakerinejad[1,2] · **Michael Maerker**[1,3]

Received: 31 August 2014 / Accepted: 11 March 2015

Abstract Soil erosion by water is a significant problem in arid and semi-arid areas of large parts of Iran. Water erosion is one of the most effective phenomena that leads to decreasing soil productivity and pollution of water resources; especially, in the Mazayjan watershed in the southwest of Fars Province gully erosion contributes to the sediment dynamics in a significant way. Consequently, the intention of this research is to identify the different types of soil erosion processes acting in the area and to assess the process dynamics in an integrative way. Therefore, we applied GIS and satellite image analysis techniques to derive input information for the numeric models. For sheet and rill erosion the Unit Stream Power-based Erosion Deposition Model (USPED) was utilized. The spatial distribution of gully erosion was assessed using a statistical approach, which used three variables (stream power index, slope, and flow accumulation) to predict the spatial distribution of gullies in the study area. The eroded gully volumes were estimated for a 7-year period by fieldwork and Google Earth high-resolution images. Finally the gully retreat rates were integrated into the USPED model. The results show that the integration of the SPI approach to quantify gully erosion with the USPED model is a suitable method to qualitatively and quantitatively assess water erosion processes. The application of GIS and stochastic model approaches to spatialize the USPED model input yields valuable results for the prediction of soil erosion in the Mazayjan catchment. The results of this research help to develop an appropriate management of soil and water resources in the southwestern parts of Iran.

✉ Michael Maerker
mmaerker@unifi.it; michael.maerker@geographie.uni-tuebingen.de

Reza Zakerinejad
reza.zakerinejad@student.uni-tuebingen.de

[1] Institute of Geography, Eberhard-Karls-University of Tübingen, Rümelinstraβe 19–23, 72070 Tübingen, Germany

[2] Faculty of Desert Studies, Semnan University, Semnan, Iran

[3] Dipartimento Scienze della Terra, Università degli studi di Firenze, Piazzale delle Cascine 4, 50144 Florence, Italy

Published online: 01 May 2015

Keywords Soil erosion · Gully erosion · GIS · Data mining · Stream power index (SPI) · USPED

1 Introduction

Soil erosion is a severe problem, especially in semi-arid and sub-humid, low- and mid-latitude areas (Lal 2001). In particular, water erosion is one of the most important factors in land degradation in large parts of Iran destroying fertile soils and agricultural land. Nearly 35 Mha of the Iranian territory is affected by different types of water erosion (FAO 1994), e.g., rill, sheet, and gully erosion.

Water erosion is a major problem because of its socioeconomic impact and the reduction in the agriculture productivity by soil loss, leaching of organic matter, and soil nutrients as well as by reducing water availability and water retention (Morgan 1995; Kirkby 2001; Poesen et al. 1996). Quantitative estimates of soil erosion by water are a key component of land-use management plans, which are designed to protect and recover soils (Bonilla et al. 2010). Additionally, the severity and spatial distribution of soil erosion are important factors to soil conservation planning and watershed management (Kumar and Nair 2006; Popp et al. 2000).

The impact of soil erosion and related sediments decreases dramatically water quality and reservoir capacity (Tangestani 2006; Kefi et al. 2011); especially, gully erosion is an important sediment source (see Poesen et al. 1996; Valentin et al. 2005; Sidorchuk et al. 2003) and hence a major threat for agricultural areas. Large parts of the southern Fars Province in Iran are affected by these soil erosion and degradation processes. The latter are related to population growth and related effects such as overgrazing, expanding agricultural land, and deforestation.

In the last decades several models were applied to assess soil erosion phenomena in Iran in a quantitative and qualitative way. Empirical models such as the Erosion Potential Method (EPM, Flanagan and Nearing 1995; Bagherzadeh and Mansouri Daneshvar 2010; Barmaki et al. 2011; Bozorgzadeh and Kaman 2012; Tangestani and Moore 2001), the Modified Pacific Southwest Interagency Committee Model (MPSIAC, Pacific Southwest Interagency Committee 1968; Ahmadi 1995; Ilanloo 2012; Mahmoodabadi and Refahi 2005; Meamarian and Esmaeilzadeh 2003; Najm et al. 2011), or the most commonly used Universal Soil Loss Equation (USLE, Wischmeier and Smith 1978; Bagherzadeh 2012; Najmoddini 2003) and its reviewed version (RUSLE, Renard et al. 1997; Arekhi et al. 2012; Asadi et al. 2011; Eisazadeh et al. 2012; Roshani et al. 2013; Vaezi and Sadeghi 2011) were applied in Iran. Moreover, numerical physically based methods, such as WEPP (Water Erosion Prediction Project, Ahmadi et al. 2011; Cochrane and Flanagan 2003; Landi et al. 2011; Nearing et al. 1989), ANSWERS (Beasley et al. 1980), or EUROSEM (European Soil Erosion Model, Morgan et al. 1998), require very detailed input data (Rusco et al. 2008), which for the southwestern parts of Iran are hardly to achieve. However, to the knowledge of the authors so far soil erosion processes were not assessed in an integrative way including gully erosion in Iran. Even though recently some models using stochastic approaches to assess gully erosion were tested elsewhere (Conoscenti et al. 2014, 2013; Zakerinejad and Märker 2014), a quantitative assessment of gully erosion phenomena do not exist on meso-scale catchments in Iran.

The Mazayjan watershed, Zarindasht, Iran, is a highly susceptible area for soil erosion and desertification because of its specific environmental and socioeconomic settings. The area is characterized by susceptible litho/pedological units, an arid climate with sporadic but intense precipitation events, as well as deforestation processes. Overgrazing and improper cultivation are additional causes of degradation and a common phenomenon in the study area. In recent years especially range land was converted to cultivated areas, even though range land generally shows a low potential to agriculture land, thus causing strong degradation and abandonment of land after a few years. Moreover, as stated by Masoudi and Zakerinejad (2010) the amount of livestock is more than two times higher than the grazing capacity. Finally, future climate change effects with predicted higher precipitation amounts may increase land degradation and soil erosion processes (Alcamo et al. 2007). Consequently, water erosion is a severe problem in this area and causes the migration of many inhabitants in recent years. Particularly, gully erosion processes and related forms and features are very common in this region. Hence, this study is aimed at identifying and quantifying the major erosion process dynamics including gully erosion. Therefore, we applied an integrated approach combining the empirical–conceptual USPED model (Mitasova et al. 1996) and the SPI index together with data mining, remote sensing, and GIS methods.

2 Study area

The Mazayjan study area (Fig. 1) is located in the Zagros Mountains of Fars Province around 32 km southwest of Zarindasht city, southwest of Iran (54°34′ to 54°44′E and 27°59′ to 28°5′N).

The landforms of the Zagros Mountains in southwest Iran reflect recent fault tectonics (Dehbozorgi et al. 2010) stretching from northwest to southwest of Iran. The study area covers ca. 966 km^2 and is drained by the Mazayjan River toward the east. The elevation ranges from 671 m to a maximum altitude of 1969 m. The average elevation of the area is 1063 m. Mean annual precipitation is around 243 mm showing a high inter-annual variability with very dry summer months (June–October) followed by short periods of heavy rainfall from December till March coming along with severe erosion and flooding events. The precipitation intensity is 23.5 and 56.1 mm h^{-1}, for a 2- and 25-year return period, respectively. In this arid environment, the hottest month is August and the coldest is February, with mean monthly maximum and minimum temperatures of 31 and 18 °C, respectively. Land use is dominated (Tab. 1) by barren land (52,782 ha), poor land (40,127 ha) and very poor range land (1758 ha), as well as agricultural areas (1168 ha), and marsh land (531 ha); especially, the barren land is characterized by very scarce vegetation of shrub and grass type and mainly concentrated in the more humid drainage lines of the pediments (see Fig. 2). Thus, vegetation might also influence the development of micro-rills. However, due to the scale of the study these processes are not taken into account.

The Mazayjan watershed is dominated by a syncline structure covered by substrates and sediments of Quaternary alluvial deposits. These deposits are eroded and transported from the mountains toward the plain in the central part of the basin. The lower Mazayjan catchment is characterized by large pediments with rills and gullies, especially located in areas with fluvio-eolian Quaternary deposits. Generally, the Mazayjan watershed is built up by conglomerates of the Plio-Pleistocence Bakhtiyari formation, Aghajari marls, Mishan

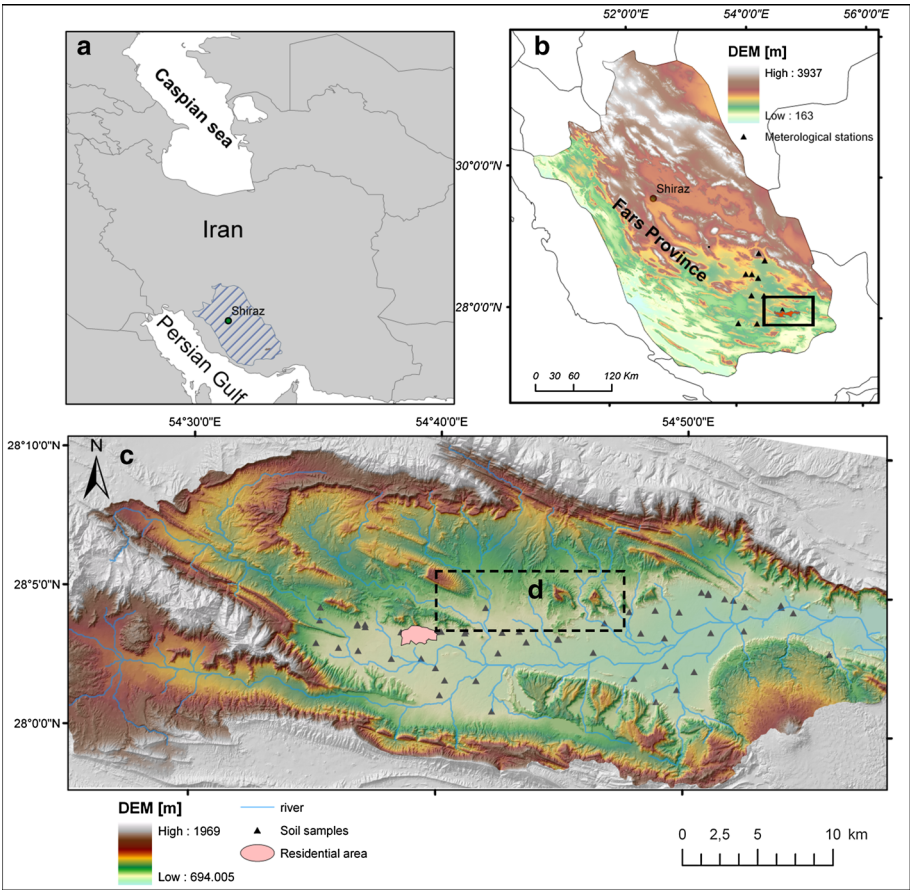

Fig. 1 Study area: Fars Province in Southern Iran (**a**). Mazayjan watershed and the locations of soil samples (**c**) and meteorological stations used for R-factor calculation (**b**). Enlarged area shown in Figs. 5, 13, and 14 (*d*)

Fig. 2 Pediment area with very poor vegetation

carbonates, and Gachsaran Anhydrite, Marl, and salt formations. The chemical properties of these deposits favor water erosion and affect also the quality of ground water. The soils of the study area are mainly Aridisols and Entisols according to soil taxonomy, and the soil moisture and temperature regimes are Aridic and Hyper Thermic. Generally the soils are not covered by stone pavements. Only in the immediate vicinity of drainage systems a higher skeleton content at the surface can be observed.

Agriculture production and animal husbandry are the main incomes in this area. The dominant agricultural products of the area are wheat, cotton, and barely. However, due to low and further decreasing productivity of soils, after some years the fields are abandoned and thus prone to erosion processes. In recent years, groundwater level decreased because of droughts and overexploitation of wells, especially for irrigation purposes.

The study area is affected by different types of water (rill, inter-rill, gully erosion) and wind erosion, especially in the eastern parts of the watershed. A major problem in this area is the large salt diaper in the southeast of the study area heavily affecting the water quality. According to the dry climate and shortage of water, the poor vegetation is sparsely distributed and also overgrazing is considered as an important cause of land degradation in this area.

3 Materials and methods

In this study the Unit Stream Power Erosion Deposition Model (USPED, Mitasova et al. 1996) was used to assess the spatial distribution of erosion and deposition processes. The parameters of this model are similar to the RUSLE model except of the topography factor that is computed by combining slope, aspect, flow direction, and flow accumulation. The USPED model predicts the spatial distribution of erosion in a steady overland flow with uniform rainfall excess conditions (Mitasova et al.1996; Mitas and Mitasova 1998; Mitasova and Mitas 2001).

The USPED model is based on the assumption that soil erosion depends on the detachment capacity and the sediment transport capacity of surface runoff. However, the USPED models do not consider the sediment yields from gullies, stream banks, and stream bed erosion (Grove and Rackham 2001). In the USPED model erosion and deposition (ED) are computed as the change in sediment flow in the direction of flow (Leh et al. 2011):

$$\mathrm{ED} = \mathrm{d}(T\cos a)/\mathrm{d}x + \mathrm{d}(T\sin a)/\mathrm{d}y \quad (1)$$

where a is the aspect of the terrain surface, dx, dy is the grid resolution, and T is the sediment flow at transport capacity. ED can be positive, indicating soil deposition, or negative, indicating soil erosion. Transport capacity is expressed as;

$$T = RKCPA^{m}(\sin b)^{n} \quad (2)$$

where R is a rainfall–runoff erosivity factor, K is a soil erodibility factor, C is a cover management factor, P is a support practice factor, b is the slope, A is the upslope contributing area, and m and n are constants. For prevailing rill erosion $m = 1.6$, $n = 1.3$, while for prevailing sheet erosion, $m = n = 1$. The USPED model was applied using Arc map 10, SAGA 2.1.0 (System for Automated Geoscientific Analysis, Conrad 2007), and ENVI 3.4 software following Mitas and Mitasova (1998).

3.1 USPED parameters

3.1.1 Rainfall erosivity factor (R)

The annual rainfall erosivity (R-factor, Renard et al. 1997) is defined as the integral measure of the amount and intensities of individual rain storms over the year that cause soil erosion (Wischmeier and Smith 1978; Mitasova et al. 1996). The R-factor in RUSLE and USPED models is calculated from the rainfall pattern or from the long-term continuous 30-min rainfall intensity (Karami et al. 2012) according to Eq. 3. The Erosivity Index (EI30), for each storm, is calculated as product of rainfall intensity of a maximum 30-min precipitation and the kinetic energy, as following:

$$R = \frac{1}{N}\sum_{1}^{N} EI_{30} \tag{3}$$

R, erosivity factor in the observed years (MJ/mm ha h years); E, total storm kinetic energy (MJ ha^{-1}); I_{30}, intensity of the maximum 30-min rainfall intensity (mm h^{-1}); N, number of observed years (Table 1).

However, the calculation of the R-factor is often difficult due to a lack of high-resolution time series (Wordofa 2011). For these reasons in many studies the annual and monthly data were used to estimate R-factor (Elsenbeer et al. 1993; Renard and Freimund 1994; Maerker et al. 2008; Karami et al. 2012).

In this study the monthly perception (January–December) was provided by the Iranian Meteorological Service for the period 1985–2006 for eight climatic stations placed around the study area (Fig. 1). Table 2 shows the climate stations that we used for the R-factor calculation. Before using the data sets, they were preprocessed to omit errors. We filled data gaps using regression relations between data of complete and incomplete stations.

To calculate the R-Factor for example the Fournier's index (Arnoldus 1980; Yuksel et al. 2008) was widely applied using mean annual perception and monthly perception according to (Eq. 4, Hu et al. 2000).

$$F = \frac{1}{N}\sum_{j=1}^{N}\left(\sum_{i=1}^{12}\frac{p_i}{p}\right) \tag{4}$$

p_i, monthly rainfall depth (mm); p, mean annual rain fall depth (mm) for rainfall stations in the same period.

However, since most of Iranian watersheds (Moussavi et al. 2012), especially in the Fars Province, are lacking sufficient high-resolution rainfall data, we tested several methods to calculate the R-factor based on monthly and annually precipitation. The calculated values finally were validated with iso-erodent maps for Iran (Sadeghi et al. 2011). Table 3 shows

Table 1 Land use/land cover (LULC) of Mazayjan watershed

LULC	Area (ha)	Area (%)
Poor range land	40,127	41.54
Very poor range land	1758	1.82
Agricultural crop	1168	1.21
Barren land	52,782	54.86
Residential area	212	0.22
Marsh land	531	0.55

Table 2 Calculated R-factor values of the rainfall stations for meteorological stations

Station	Longitude (decimal degree)	Latitude (decimal degree)	Elevation (m)	Mean annual rainfall (mm)
Darb ghale	54.23	28.55	1430	344.0
Ghozan	54.27	28.49	1300	347.6
Hajiabad	54.25	28.22	1060	248.3
Brak	53.09	28.39	870	354.0
Farag	55.12	28.22	890	213.5
Khasoe	54.23	28.33	1070	241.5
Layzgan	54.58	28.41	2000	492.9
Larstan	54.19	27.38	860	270.3
Avaz	54.00	27.46	860	236.1

Table 3 Commonly applied equations to estimate erosivity factor in study area

Equation	Parameters	Author(s)	CV	SD	R^2
$R = 0.524\left(\sum_{i=1}^{12} \frac{p_{ij}^2}{p_j}\right)^{159}$	p_{ij} total precipitation (mm) of the generic month i of the year j. P_j total precipitation (mm) of the year j	Ferro et al. (1991)	0.45	448.80	0.84
$Y = 50.0427X - 47.683$	X = maximum daily precipitation (mm)	Sadeghifard et al. (2004)	0.30	172.10	0.75
$R = 0.0483\ P_a^{1.61}$ $P_a \leq 850$ mm $R = 587.8 - 1.249\ Pa + 0.004105\ P_a^2$ $P_a > 850$	Pa denotes annual rainfall amount (mm).	Renard and Freimund (1994)	0.51	241.70	0.81
$R = 0.264MFI^{1.50}$	Modified Fournier	Renard and Freimund (1994)	0.43	90.50	0.31
$R = (0.07397 \times F\ 1.847)/17.2$ $F < 55$ $R = ((95.77 - (0.681 \times F)) + (0.477 \times F^2)))/17.2$ $F \geq 55$	F; Fournier index	Renard and Freimund (1994)	0.39	768.23	0.48

the utilized equations as well as a comparative statistics with R^2, coefficient of variation (CV), and standard deviation (SD). Subsequently, we calculated the R-factor for all stations and generated R-factor layers for the whole area using a spatial regression between R-factor and elevation as shown in Fig. 2 (Arekhi et al. 2012; Asadi et al. 2011; Arekhi and Niazi 2010).

3.1.2 Crop and management factor (C)

The C-factor represents the effects of (1) plants above the soil surface, (2) the below-ground biomass, (3) residuals of crops on the surface, and (4) special effects of former

Table 4 C-factor values used in the USPED model

LULC	C-factor	Reference
Poor range land	0.25	Feiznia and Ahzan (2004)
Very poor range land	0.33	Feiznia and Ahzan (2004)
Agricultural crop	0.43	Adediji et al. (2010)
Barren land	0.60	BCEOM (1998)
Residential area	0.00001	Adediji et al. (2010)
Marsh land	0.01	BCEOM (1998)

Table 5 Accuracy of land use/land cover (LULC) from Landsat image 2006 in Mazayjan watershed

Land use	Users accuracy	Producers accuracy	Kappa coefficient
Poor range land	0.79	0.73	0.62
Very poor range land	0.79	0.81	0.74
Agricultural area	0.89	0.86	0.84
Barren land	0.82	0.79	0.74
Marsh land	0.93	0.94	0.91
Overall accuracy	0.88		

agriculture residues on soil erosion (Maerker et al. 2008; Wang et al. 2003). In other words the C-factor indicates how vegetation and land-use management affect soil erosion. The C-factor is often estimated as a function of land use and land cover (LULC) (Maerker et al. 2008; Pelacani et al. 2008; Terranova et al. 2009; Renard et al. 1997; Yuksel et al. 2007). For different land-use/land-cover classes C-factor values can be attributed based on existing published studies. The C-factor can also be derived using vegetation indices based on satellite image analysis (Kouli et al. 2009). Table 4 shows the land-use classes and the attributed C-factor values we assigned (Adediji et al. 2010; BCEOM 1998; Feiznia and Ahzan 2004). The land-use/land-cover classification was derived using a Landsat ETM images from March 2006 and a maximum likelihood classification implemented in ENVI 3.4. Subsequently, a majority filter was applied on the classified data in order to reduce noise and artifact pixels. The final land-use/land-cover map was validated in the field. Error matrices and Kappa coefficient were calculated as shown in Table 5. The C-factor values vary from 0 to 1 (nondimensional), reflecting the effect of cropping and land cover to protect soil from rainfall and runoff erosion. Values tending to 0 reduce soil loss.

3.1.3 Soil erodibility factor (K)

The erodibility of a soil is characterized by inherent soil resistance to both detachment and transport, by raindrop impact and surface flow processes (Bryan 2000; Lal 2001; Onori et al. 2006). The soil erodibility factor or K-factor (in t h MJ^{-1} mm^{-1}) accounts for the influence of soil properties on soil loss during storm events on upland areas (Onori et al. 2006). The soil erodibility factor is usually derived using nomographs and/or formulae and is determined by soil texture, soil organic content, soil structure, and infiltration capacity (Wischmeier and Smith 1978). In this study, the K-factor was estimated according to Renard et al. (1997):

$$K = 7.594\left\{0.0034 + 0.0405\exp\left(\left(-\frac{1}{2}\cdot\frac{\log D_g + 1.659}{0.7101}\right)^2\right)\right\} \quad (5)$$

K, soil erodibility factor (t ha^{-1} MJ^{-1} mm^{-1}); Dg, geometric mean particle diameter (mm); f_i, primary particle size fraction; m_i = arithmetic mean of the particle size limits of that size.

To calculate the mean particle diameter, we used the percentage of clay, silt, and loam (Tables 6, 7, 8).

In this research 52 soil samples (Fig. 1) were collected and analyzed for soil texture using a standard analytical method (Gee and Bauder 1986). Soil samples were selected using a catena-based sampling design (Conacher and Dalrymple 1977). Soil texture and organic matter (OM) prevalently affect the soil water content and hence the amount of runoff (Saxton and Rawls. 2006). Moreover also electric conductivity (EC) and sodium absorption rates (SAR) are analyzed. High EC and SAR values facilitate soil erosion and favor especially piping processes (Faulkner et al. 2004).

3.1.3.1 Spatial Prediction of K-factor using stochastic modeling The spatial distribution of K-factor was estimated using a stochastic gradient boosting technique (TreeNet, Salford Systems) (Elith et al. 2008; Friedman 1999). Predictor variables are based on terrain parameters and landsat image spectral bands. TreeNet has several advantages since it is resistant to over-training and outliers (Friedman 2002). Since topography controls both hydrological and soil processes (Amundsen et al. 1994; Sariyildiz et al. 2005; Seibert et al. 2007), the topography data can be utilized to predict soil types or soil properties (Behrens et al. 2005). In this model, different topographic indices (Tab. 6) were extracted from a DEM with 5-m resolution. Laboratory-estimated K-factor values are used as the dependent variable.

The DEM is based on 19 stereo aerial photographs from 1994 of 1:20.000 scale provided by the Iranian Cartographic Centre. With the software AGISOFT we generated the

Table 6 Topographic indices used for environmental predictors in TreeNet model

Topographic indices	Method
Watershed sub bins	Olaya and Conrad (2009)
Wetness index	Olaya and Conrad (2009)
Stream power	Olaya and Conrad (2009)
Slope	Zevenberg and Thorn (1987)
LS-factor	Olaya and Conrad (2009)
Profile curvature	Olaya and Conrad (2009)
Plan curvature	Zevenberg and Thorn (1987)
Catchment area	Olaya and Conrad (2009)
Curvature classification	Dikau (1989)
Curvature	Zevenberg and Thorn (1987)
Convergence index	Köthe and Lehmeier (1993)
Channel network base level	Olaya and Conrad (2009)
Channel network	Olaya and Conrad (2009)
Aspect	Zevenbergen and Thorne (1987)
Altitude above channel network	Olaya and Conrad (2009)
Elevation	Preprocessed in ArcGIS9.2

Table 7 Frequency ratio values of gully areas and soil erosion/deposition classes in study area

Soli Erosion/ Deposition	Area (ha)	Erosion and deposition areas (%) (P)	Gully erosion points*	Gully erosion points % (G)	Frequency ratio G/P
Very high erosion	33,113.07	32.26	1020	4.33	0.12
High erosion	4893.74	7.06	1000	4.24	0.83
Medium erosion	7363.81	7.62	2000	8.49	1.11
Low erosion	6190.18	6.40	1890	8.03	1.25
Very low erosion	11,898.44	10.31	3450	14.66	1.19
Stable	11,898.44	3.77	6380	27.11	7.18
Very low deposition	3645.74	7.75	2440	10.36	1.80
Low deposition	5562.88	2.33	1500	6.37	2.72
Medium deposition	2617.74	2.70	1750	7.43	2.74
High deposition	1668.31	1.72	1020	4.33	2.51
Very high deposition	17,422.24	18.02	1080	4.58	0.25

* Each point corresponds to one pixel or 25 m^2 gully areas (5*5 m^2)

Table 8 Categories of soil loss in Mazayjan watershed

Erosion/Deposition (categories)	Erosion/Deposition (t ha^{-1} $year^{-1}$)	Area (ha)	Total area (%)
Very high erosion	<−30	27,241.2	28.2
High erosion	−20 to −30	8887.2	9.2
Medium erosion	−10 to −20	5989.2	6.2
Low erosion	−5 to −10	3284.4	3.4
Very low erosion	−1 to −5	5699.4	5.9
Stable	−0.1 to 0.1	5989.2	6.2
Very low deposition	0.1 to 5	5119.8	5.3
Low deposition	5–10	2898	3.0
Medium deposition	10–20	3477.6	3.6
High deposition	20–30	9466.8	9.8
Very high deposition	>30	18,547.2	19.2

DEM using 60 ground control points (GCP) taken in the field with a DGPS. The DEM was georeferenced using an UTM projection. The DEM was preprocessed with low-pass filtering (3*3 filter) to extract artifacts and errors such as local noise and terraces. Thereafter, it was hydrologically corrected to eliminate sinks using the algorithm proposed by Planchon and Darboux (2001). Finally, the spatial relations between dependent and independent variables revealed by the TreeNet model are used to predict the spatial distribution of the K-factor (Fig. 3).

To evaluate the performance of the TreeNet model the data were randomly divided into training (80 %) and a test data subset (20 %). The model results were evaluated using the receiver operating curve characteristics (ROC) for training and test data. The ROC integral values range between 0 and 1. A value near to 1 indicates high model accuracy, and values of 0.5 show a random model. According to Hosmer and Lemeshow (2000) ROC integral or area under curve (AUC) values exceeding 0.7/0.8/0.9 indicate acceptable/excellent/outstanding predictions.

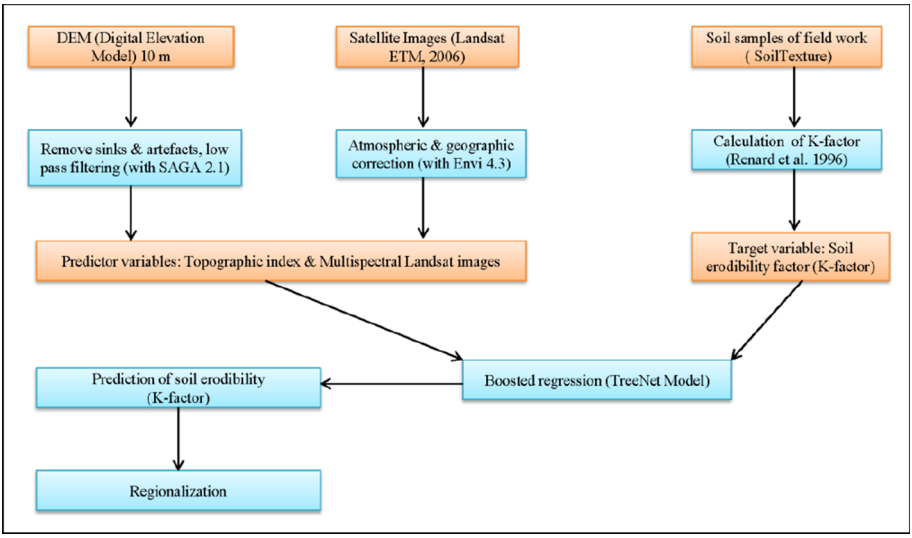

Fig. 3 Flowchart of the applied methodology for the prediction of K-factor used in the USPED model

3.1.4 Support practice factor (P)

The support practice (P) is related to management practices such as contouring and terracing to reduce the soil erosion. In other words, the P-factor describes the impact of management practices on average annual of soil erosion (Arekhi et al. 2012).

The values range between 0 and 1, and for areas with no support practice, the P-factor value is set to 1 (Simms et al. 2003). According to our survey in the study area we have identified no practice management to be considered, and thus, we assumed a P-factor value of 1 for the entire study area.

3.2 Gully erosion assessment using a steam power index (SPI) threshold

Gully erosion is a very intensive type of water erosion in southwestern Iran. As already mentioned the USPED model can only assess rill and inter-rill or sheet erosion processes. However, gully erosion affects large parts of the study area. In order to assess this deep linear gully erosion features we applied a stream power index (SPI)-based approach with a flow accumulation threshold. The SPI indicates the erosive power of flowing water over a specific area (Tagil and Jenness 2008; Kakembo et al. 2009; Moore and Wilson, 1992) and thus describes the potential energy to entrain sediments (Shruthi et al. 2011). The SPI (Moore and Wilson 1992) as one of the secondary terrains attributes (Wilson and Gallant 2000) is calculated as follows:

$$\mathrm{SPI} = \ln(A_s * \tan \beta) \tag{6}$$

where A_s is specific catchment area and β is slope in degree.

The SPI values highlighted distinct preferential topographic areas for gully formation (Kakembo et al. 2009). This index has been calculated from the DEM with 5-m resolution based on the 1994 stereo aerial photographs 1:20.000 scale provided by the Iranian Cartographic Centre. Consequently, the DEM was generated before we mapped the gully

Fig. 4 Gully erosion features after a precipitation event

features. Actually, in many studies the relations between slope and flow accumulation were utilized to estimate the thresholds of gully initiation (see, e.g., Kheir et al. 2007; Tagil and Jenness 2008; Wilson and Gallant 2000). To calibrate the SPI approach we identified threshold values for SPI around existing gully heads. Therefore, we used high-resolution satellite images from Google Earth (GE). The available GE images for the Mazayjan watershed are built on Spot images with a 2.5-meter resolution. We identified 49 gully head locations based on field survey and using the available GE images. However, the absence or scarcity of vegetation facilitates the mapping procedure (Figs. 2, 4).

To extract a SPI threshold value for gully erosion we overlay the gully headcut areas with the SPI raster map (Fig. 5). Although there are different thresholds for gully erosion initiation, e.g., due to land use, soil character, and hydraulic conductivity, the study area is very homogenous, and hence, the main controlling factor is the topography. In the study

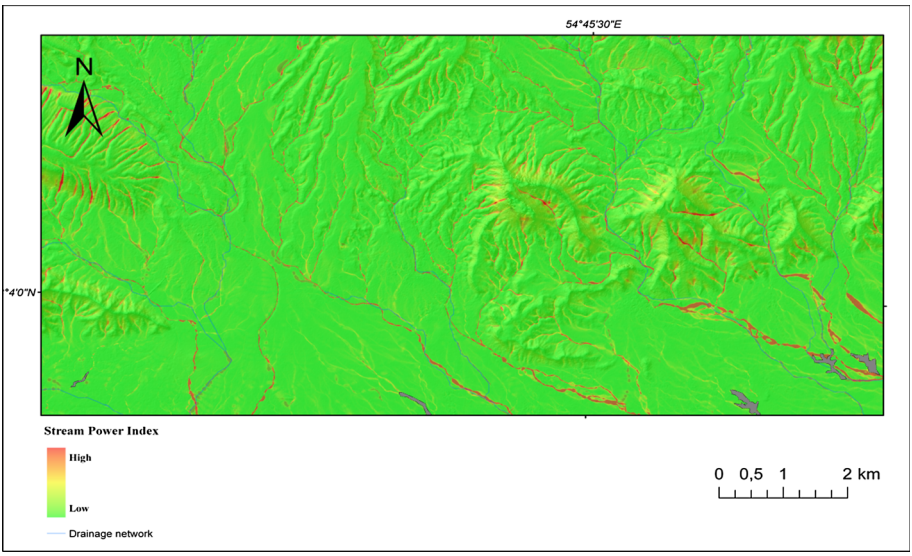

Fig. 5 Stream Power Index for the zoomed area in *dark gray*: gully areas (enlarged area (*d*) shown in Fig. 1)

area 12 gullies out of 49 were selected to determine the rate and expansion for a 7-year period. GE provides SPOT images from 2003 to 2009. Based on these images, the expansion of head cuts was estimated by digitizing the gully area for the two time steps. During a field survey in 2013 we measure the gully depth and growth areas in order to validate the GE image analysis. According to the satellite images, aerial photos from 1996, and field survey the gully features are mainly located in the flat and low sloping areas. Therefore, we limit our SPI approach to these areas using a low flow accumulation threshold of 100 ha and a maximum slope of 35°. We converted the eroded gully volumes to tons per hectare using a soil bulk density value of 1.23 g/cm^3 (Kompani-Zare et al. 2011). To get the yearly gully erosion rates we divided the value by the duration of our observation period (7 years). We integrate the gully erosion estimated for the single spatial units into the USPED model by adding the amount of sediments eroded by gullies to the sediment flow at sediment transport capacity.

4 Results and discussions

4.1 USPED–factors

According to the USPED model algorithm the input data (R, K, C, P and topographic factor) were multiplied with the Raster Calculator in ArcGIS 10.0 to get the erosion/deposition rates in t ha^{-1} yr^{-1} for each grid cell.

According to Table 3, the best equation to calculate the R-factor is the one developed by Sadeghifard et al. (2004) for the arid climate in south of Iran. Consequently, we applied this equation to estimate the erosivity factor for the Mazayjan watershed. Since the relationship between elevation and average annual precipitation shows a high correlation ($R^2 = 0.89$), we used elevation to regionalize the R-factor for the Mazayjan watershed ($R^2 = 0.75$) (Fig. 6). The obtained values (Fig. 7) range from 212.6 to 424.6 MJ mm/ha year^{-1}. The average values for the Mazayjan watershed amount to 265.2 MJ mm/ha year^{-1}. The spatial distribution of R-factor values for the Mazayjan watershed is presented in Fig. 7. In particular, high precipitation values occur along the ridges of this basin.

According to the soil laboratory analysis soil texture is dominated by silt loam and sandy loam and thus is highly susceptible to soil erosion. The amount of organic matter in all samples was <2 %. Soil organic matter reduces the erodibility of soil. In many arid and semiarid areas soil organic matter is low due to scarce vegetation, and hence, soil is more susceptible to erosion. Particularly in the southwest of Iran, due to arid climate and lack of

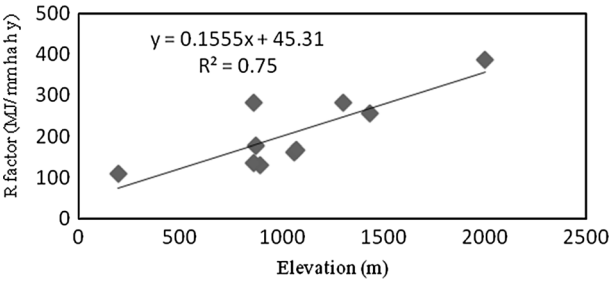

Fig. 6 Relationship between R-factor and elevation

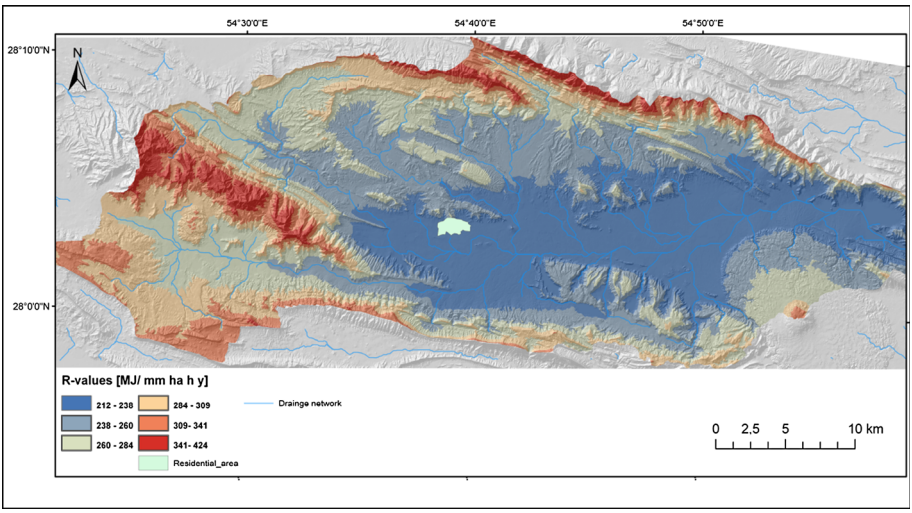

Fig. 7 R-factor layer of Mazayjan watershed

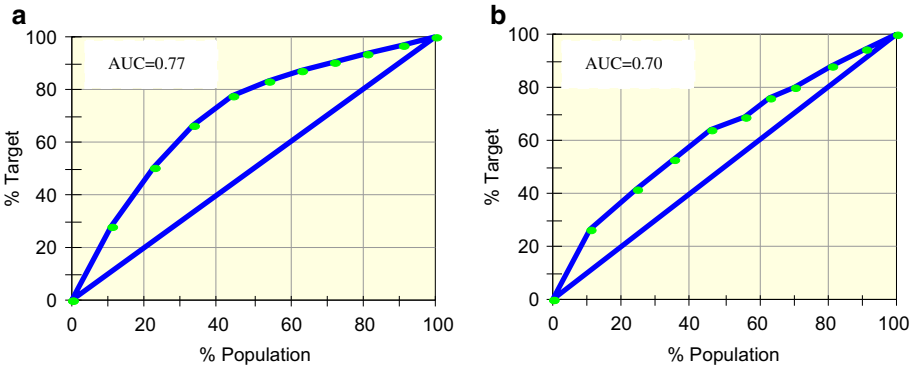

Fig. 8 ROC diagram and AUC values for K-factor. *Left*: train data set; *right*: test data set

organic matter wind erosion affects large areas. Moreover, the laboratory analysis shows that the EC and SAR values of soil samples indicate high sodium contents that amplify gully erosion and the degradation of rangeland (Shahrivar et al. 2012; Masoudi et al. 2006). The stochastic modeling of the K-factor values based on the soil samples (dependent variable) and on terrain parameters and Landsat spectral bands (independent variables) was validated internally using the ROC integral (area under curve, AUC) for training and testing data. According to Hosmer and Lemeshow (2000) the K-factor model shows an acceptable performance with AUC integrals of 0.77 and 0.70 for training and testing data set, respectively (Fig. 8). Figure 9 shows the variable importance. The most important factors are slope and vertical distance to channel network. Finally we applied the TreeNet model to predict the spatial distribution of the K-factor as shown in Fig. 10. High K-factor values are related to the plain areas with flat slope (<2 %) and to the vicinity of the channel network in the central part of watershed.

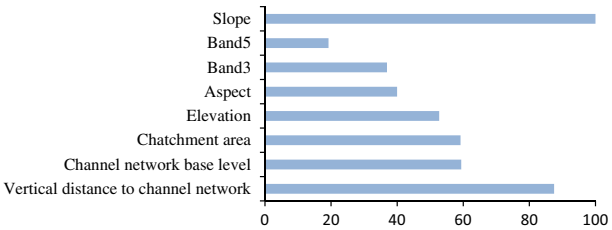

Fig. 9 Variable importance obtained by the boosted regression tree model for soil erodibility (values in %)

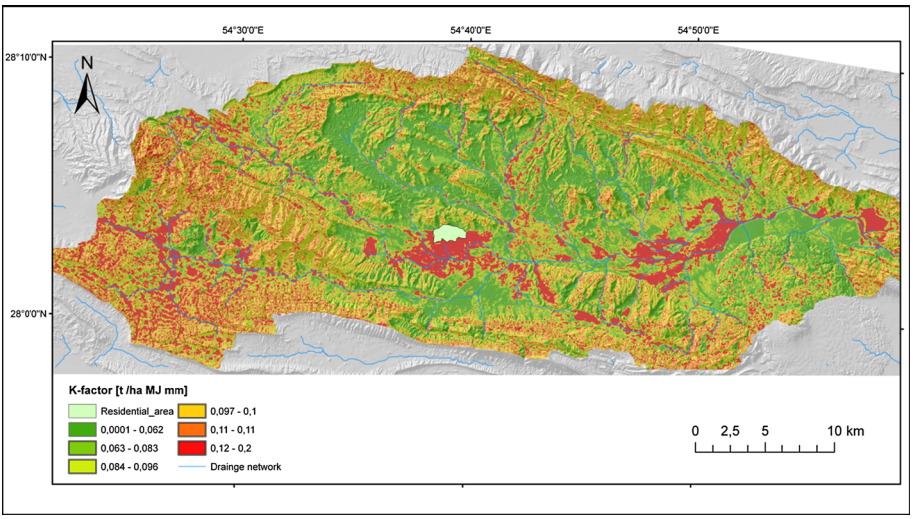

Fig. 10 K-factor layer of Mazayjan watershed

Soil erodibility values vary from 0.11 t ha MJ^{-1} mm^{-1} in the northern and northeastern part of the study area with more sandy loam and sandy clay soils, to 0.32 t ha MJ^{-1} mm^{-1} in the southwestern and southeastern part of the area with silty loam soils. The total mean is 0.11 t ha MJ^{-1} mm^{-1} with a standard deviation of 0.02 t ha MJ^{-1} mm^{-1}. According to the K-factor map low K-factor values coincide with the Asmari-Jahrom (AS-Ja) and the Tarbur formation that are relatively resistant to water erosion (Feiznia 2000). The high values of K-factor are more related to Quaternary formations and alluvial deposition.

We derived C-factor values using the land-use map. The classification result based on Landsat images was validated using field data. In this research some accuracy estimating indexes are shown, such as overall accuracy, user's accuracy, producer's accuracy and kappa coefficient (Table 5). Accuracy analysis was completed by means of a confusion or error matrix. This method relates the numbers of classified pixel in the assigned classification to the ground truth data (Congalton and Green 1999). In addition, the Kappa coefficient accuracy for all classes was higher than 0.60. Finally, this index is used to calculate the classification. High values of the Kappa coefficient indicate higher reliability of the classification results. The overall accuracy of the supervised classification of LULC is 88 %. According to Table 4 C-factor values were attributed to the singles LULC classes. Values range from 0 to 1 with bare rocks and no vegetation having values of 1. In the Mazayjan watershed the vegetation is poor due to the arid climate and over grazing;

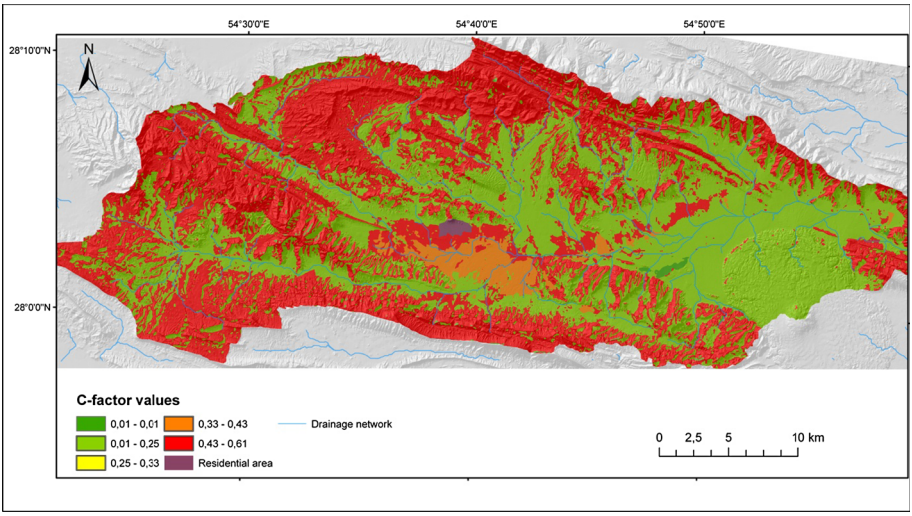

Fig. 11 C-factor layer of Mazayjan watershed

especially, the southwest of the study area is characterized by no vegetation at all or scarce shrubs. The major LULC in this area is poor and very poor vegetation with C-factor values of 0.23. The rest of the study area is covered with agriculture land use having C-factor values of 0.43. Figure 11 shows the maximum amount of C-factor values coinciding with barren areas in ridge positions in the north and southwest of the watershed, whereas the lowest values are related to the areas with scarce vegetation. The artificial and rural area was masked in the C-factor map. The mean C-factor value is 0.15 with a standard deviation of 0.12.

4.2 Distribution of Gully erosion processes

In this study the gully head cut locations were identified using GE image interpretation. We set up a regression model between headcut location and SPI values using a set of 12 mapped gully headcut locations. Subsequently, the gully erosion rates were estimated by mapping the growth rates of the 12 gullies over a 7-year time period. As already pointed out by other studies there is a strong relationship between catchment area and slope and turbulent concentrated runoff forming longitudinal deep incisions (Kakembo et al. 2009; Nazari Samani et al. 2009; Poesen et al. 1996; Vandekerckhove et al. 2001). As illustrated in Fig. 12 the regression between the volume of soil losses for each gully location and SPI values shows a very good fit ($R^2 = 0.84$). Consequently, we can use a threshold value of SPI to identify potential gully initiation points. Extreme high values of SPI are related to the stream network in the flat areas.

In the study area gully erosion threads the agricultural land and infrastructures like roads. The SPI threshold characterizing gully erosion ranges between 100 and 1700 in different parts of this catchment. SPI values higher than 1700 indicate stream network, while values of less than 100 display areas not affected by gullying. In fact using this threshold, we are also able to compare potential and actual gully erosion (Kakembo et al. 2009). Figure 5 shows that the susceptible zones are prevalently in the low sloping and

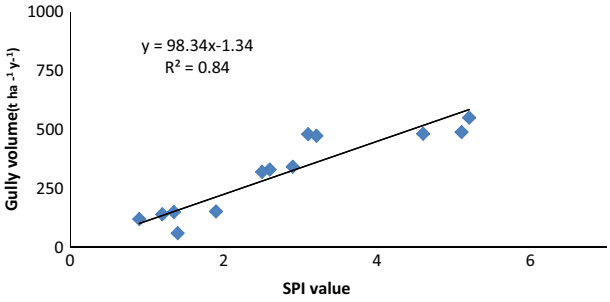

Fig. 12 Relationship between SPI values and gullies volumes for 2003–2009 [t ha^{-1} year^{-1}]

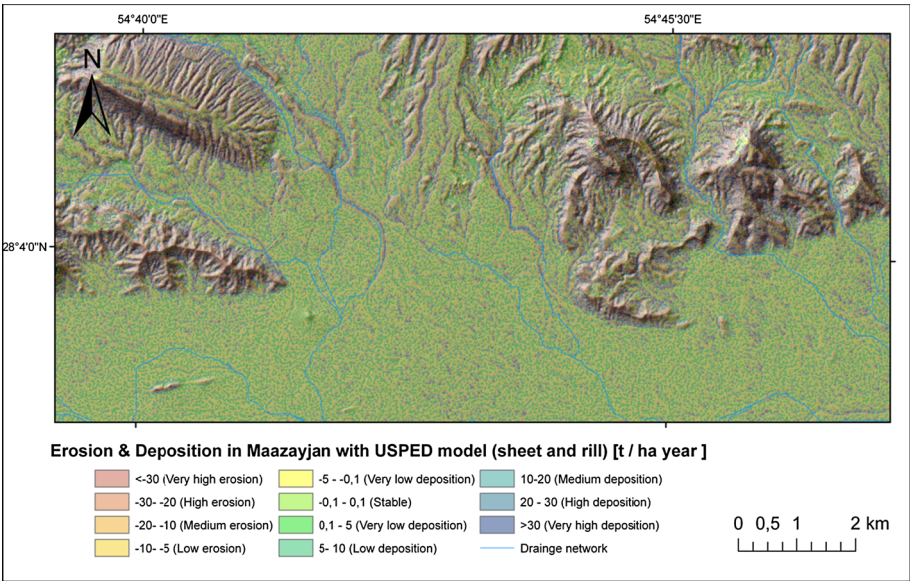

Fig. 13 Predicted soil erosion and deposition for the Mazayjan [t ha^{-1} year^{-1}] derived with the USPED model for enlarged area (*d*) shown in Fig. 1)

pediment areas. However, the USPED model simulates for these areas low soil loss or instead deposition (Fig. 13).

4.3 Comparison of the USPED model and the gully erosion approach

We compared the model results of the USPED erosion/deposition values with the gully sample points creating a Frequency ratio. As illustrated in Figs. 13 and 14, the gully features are frequent in bare soil in pediment and glacis areas. However, the steeper areas around the Mazayjan plain show no predominant gully erosion phenomena due to shallow soils and small specific catchment areas. Table 7 shows the frequency ratio for gully points and the respective soil categories. According to this table the frequency ratio for two classes of very high erosion and deposition is 0.12 and 0.25, respectively, while the low and very low erosion are higher than 1. The frequency ratio clearly demonstrates that gully

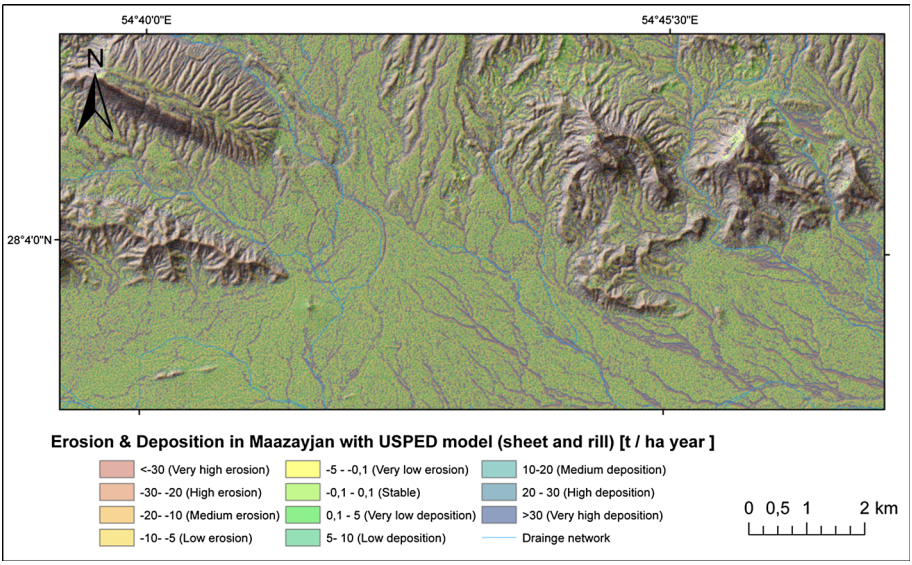

Fig. 14 Spatial distribution of soil erosion and deposition in the Mazayjan watershed [t ha^{-1} $year^{-1}$], based on the integrated USPED/SPI approach for the enlarged area (*d*) as shown in Fig. 1

erosion is completely underestimated by the USPED model. This was already documented for RULSE-type models (Biesemans et al. 2000; Le Roux et al. 2008).

4.4 Integrated assessment of erosion processes in the Mazayjan basin

In order to get the total amount of soil eroded, transported, and deposited by sheet (rill/inter-rill erosion) and gully erosion processes we utilized the USPED model adding the volumetric contribution of the deep linear gully erosion processes estimated with the SPI approach as layer in the calculation of the transport capacity.

According to field work and aerial photo interpretation gullies generated by overland flow occur in abandoned land, rangeland and agricultural areas.

4.5 Soil erosion/deposition potentials

According to Fig. 13 and Table 7 more than 50 % of the area is affected by high to very high erosion and deposition process intensities. The stable areas and low erosion and deposition zones cover about 21 % of the area. However, some of the mapped and predicted gully processes are located in the stable and low intensity soil erosion classes. The extreme values are characterized by steep slopes in ridge positions in the northern and western parts of the basin.

Figure 14 shows the final map combining the USPED (for rill and sheet) with the SPI and flow accumulation approaches (for gully erosion) for the entire study area. This map shows that the flat areas are highly susceptible to gully erosion, while the USPED model shows low sheet erosion susceptibility for these areas (Fig. 13). In other words large parts of the flat areas are very prone to gully erosion.

Table 8 illustrates the soil erosion and deposition values classified in 11 classes for the integrated model as follows: Stable areas range between −0.1 and 0.1 t/ha year, values <− 0.1 t/ha year characterize erosion, and values with more than 0.1 t/ha year describe deposition/sedimentation processes (De Rosa 2005). Consequently, areas with a higher soil loss rate with respect to the tolerable one of 10 t/ha year (see, e.g., Ahmadi 1995; Pradhan et al. 2012; Le Roux et al. 2008) fall into the moderate and high soil loss classes.

According to the combined final map of erosion deposition processes modeled with USPED and including the gully erosion processes derived by SPI (Fig. 14) round about 17.5 % of area is stable or characterized by very low erosion or deposition classes. Very high erosion values cover 28.2 % of the area, whereas 19.2 % of the area is related to deposition processes. The spatial variation of erosion/deposition processes show more intensive processes in the north, northwest, and east part of the study area that are generally associated with the steeper relief of the mountain ranges (Table 9). Area with high deposition is mainly located in the central part and along the drainage networks because of low transport capacities. However, the plain areas are characterized by high SPI values due to large specific catchment areas and hence are more susceptible to gully erosion. Areas of low erosion and deposition tend to coincide with flat areas showing low soil erodibility and better vegetation cover.

The integrated USPED/SPI approach shows that more than 43 % of the area is affected by soil erosion with more than 10 t ha^{-1} $year^{-1}$. Moreover, the average value of erosion with 37.6 t ha^{-1} year is higher than the annual average of soil erosion (33 t ha^{-1} $year^{-1}$) for Iran (Hoseini and Gorbani, 2005; Omidvar 2010). Furthermore, the average predicted soil loss rate for the study area is four times higher than the mean global soil loss (Omidvar, 2010). However, the integrative soil erosion maps (Fig. 14) show similar values reported by other studies using the PASAC and EPM model in southwest of Iran (Nikeghbal and Rafati 2009; Tangestani 2006).

Table 9 Error matrix showing predicted erosion and observed erosion on pixel basis

Classes	Slight and low erosion [no. of pixel]	Moderate erosion [no. of pixel]	Severe and very severe erosion [no. of pixel]	Row total	Omission error*	Commission error**
Stable, low, and very low erosion/ deposition classes	34	14	5	53	35.84 %	16.98 %
Moderate erosion/ deposition classes	5	32	10	47	34.42 %	29.78 %
High and very high erosion/ deposition classes	4	6	41	51	19.60 %	29.40 %
Overall Accuracy	0.70	–	–	–	–	–

Predicted erosion intensity is compared with values based on field survey and qualitative IMDPA model; Masoudi and Zakerinejad (2011)

* Omission error: Sample points for each pixel that has not been correctly classified and has been

Omitted from the category for each class

** Commission error: Sample points that have been inaccurately commissioned into a different category

The Mazayjan basin area is characterized by surrounding high mountain ranges with steep slopes and thus shows intensive erosion processes. In fact steeper slopes increase runoff velocity, detachment, and transport of sediments (Kefi et al. 2011; Wordofa 2011). Therefore, in the affected areas priority should be given to increase vegetation cover to decrease runoff velocities and protect soils. The deposition areas mainly concentrate close to or along the stream networks. These areas are characterized by high erodibilities of the substrates and turbulent runoff with the consequent evolution of gully networks.

4.6 Validation of the integrated USPED/SPI approach

The validation of soil loss predictions with numerical models is often difficult due to a lack of measured data to compare to (Gobin et al. 2004; Tangestani 2006). In some research the USLE-based erosion models are validated using landslide initiation points (Pradhan et al. 2012), ephemeral gully headcut locations (Suriyaprasit 2008), or simple field survey or qualitative models (Tangestani 2006; Kefi et al. 2011); especially, the assessment of soil loss through ground survey particularly in areas with complex terrain or restricted accessibility due to property rights is limited (Jianping et al. 2012).

The accuracy of numerous empirical soil modeling studies is difficult to validate in many basins of Iran due to the lack of gauging stations (Safamanesh 2004). Therefore, in this research the validation of the final integrated soil erosion/deposition map was performed using a combined approach based on aerial photos interpretation, field survey, and satellite image interpretation utilizing freely available high-resolution satellite images from GE. Additionally, we compared also to a qualitative model applied in the area (Masoudi and Zakerinejad 2011).

In this study we validate the soil loss of the prediction model with the field observation map of water erosion (see Masoudi and Zakerinejad 2011). The validation is illustrated as error matrix (Table 9). The error matrix contains a simple pixel-to-pixel comparison between predicted and observed soil loss. The error matrix in Table 9 shows omission, commission error, and overall accuracy for each class. According to this table the omission error is higher for the stable and low soil erosion classes than for severe and very severe soil erosion classes. The overall accuracy of the water erosion prediction map compared to the field observations is 77 %. Generally, the result of this validation procedure shows a high accuracy of the estimated soil loss by our integrated model. However, especially in flat parts of the study area the DEM is characterized by some noise and artifacts that affected the USPED modeling and also the SPI calculation. However, the validation procedure shows that our approach gives a proper picture of the spatial distribution of sheet erosion, gullying, and deposition processes. Moreover, also the process intensities are simulated adequately as shown in (Fig. 14).

5 Conclusions

During recent years, the role of water erosion as one of the land degradation factors in arid and semi-arid areas of large parts of Iran has increased (Ahmadi 2006; Hoseini and Gorbani 2005; Masoudi et al. 2006). In our study we applied a combined approach using

the USPED model, the SPI, and a flow accumulation index in the southwest of Iran to characterize areal rill/inter-rill (sheet) erosion processes, gully erosion processes, and deposition processes. To the knowledge of the authors, this is the first attempt integrating different erosion processes and deposition dynamics in Iran.

The parameters utilized in this integrated model consist of (1) the erosivity factor (R-factor) calculated from monthly rain fall data, (2) the erodibility factor (K-factor) derived by data mining techniques, (3) the land-use factor (C-factor) delineated from Landsat ETM land-use classification, (4) the topography factor derived from a DEM with 10-m resolution, and finally (5) the SPI and flow accumulation to identify gullied areas. The results of this research show the spatial distribution of soil erosion and deposition processes. Thus, the integrated model is a useful tool to indentify susceptible areas for erosion and deposition processes. Hence, the obtained results consent a better land management and land-use planning in order to control soil loss.

In many previous studies in Iran qualitative models like IMDPA or MPSIAC were used for the assessment of water erosion processes as one important indicator of desertification (Ahmadi 2006; Masoudi et al. 2006; Masoudi and Zakerinejad 2010). Consequently, the proposed methodology provides spatially distributed information about process intensities and thus outperforms the qualitative models, especially in regard to land-use planning purposes. The application of a threshold value of SPI together with an estimate of gully volume using GE images is a simple but powerful tool to predict gully locations and gully erosion intensities.

In the study area soil loss is concentrated especially in the abandoned agricultural areas. The protection of bare soil to reduce soil loss should be ensured by appropriate cultivations (Lesschen et al. 2007). According to the results a large part of severe erosion occurs in the steep areas in the north and northwest of the study area. Main gully erosion activity is concentrating in the low sloping pediment and alluvial areas. Agricultural cultivations may change the land cover, leading to poorer vegetation cover or bare land, especially after harvest and thus increase erosion processes and land degradation. Also overgrazing even though not directly considered in the modeling procedure, but via the C-factor, and improper cultivation are two main causes of degradation processes in southwest of Iran and especially in Fars Province. In fact socioeconomic factors have an important role on land degradation and soil loss in this area; therefore, it is suggested to assess these factors in more detail maybe with questionnaires about land-use practices and livestock farming on farmers level.

Acknowledgments The authors would like to thank the Iranian Ministry of Science and Technology for providing the fellowship of Mr. Zakerinejad. Moreover, we would like to thank the Heidelberg Academy of Sciences and Humanities for field work and travel funding and the Department of Geography at University of Tübingen, Germany for hosting the research activities and providing laboratory and computer facilities. Finally we would like to thank also the Marie Curie EU-IRSES project entitled FLUMEN for support and assistance. The authors also express their gratitude to the Haseb Karaji Company in Iran, for providing the aerial photos and climate data for this research.

References

Adediji A, Tukur AM, Adepoju KA (2010) Assessment of Revised Universal Soil Loss Equation (RUSLE) in Katsina Area, Katsina State of Nigeria using remote sensing (RS) and geographic information system (GIS). Iran J Energy Environ 1(3):255–264

Ahmadi H (1995) Applied geomorphology. Tehran University Publication, Iran, p 613 (in Persian)

Ahmadi H (2006) Iranian model of desertification potential assessment in (East of Esfahan). Faculty of Natural Resources University of Tehran (in Persian)
Ahmadi H, Taheri S, Feiznia S, Azarnivand H (2011) Runoff and sediment yield modeling using WEPP in a semi-arid environment (Case study: Orazan Watershed). Desert 16(2011):5–12
Alcamo J, Flörke M, Märker M (2007) Future long-term changes in global water resources driven by socio-economic and climatic changes. Hydrol Sci J 52(2):247–275
Amundsen R, Harden JW, Singer MJ (1994) Factors of soil formation: a fiftieth anniversary perspective. Soil Sci Soc Am J, Special publication, 33
Arekhi S, Niazi Y (2010) Investigating application of GIS and RS to estimate soil erosion and sediment yield using RUSLE (Case study: upper part of Ilam Dam Watershed, Iran). J Water Soil Conserv 17(2):1–27 (in Persian)
Arekhi S, Darvishi Bolourani A, Shabani A, Fathizad H, Ahamdyasbchin S (2012) Mapping soil erosion and sediment yield susceptibility using RUSLE, remote sensing and GIS (Case study: Cham Gardalan Watershed, Iran). Adv Environ Biol 6(1):109–124
Arnoldus HMJ (1980) An approximation of the rainfall factor in the universal soil loss equation. In: De Boodt M, Gabriels D (eds) Assessment of erosion. Wiley, Chichester, pp 127–132
Asadi H, Vazifehdoost M, Moussavi A, Honarmand M (2011) Assessment and mapping of soil erosion hazard in Navrood watershed using revised universal soil loss equation (RUSLE), geographic information system (GIS) and remote sensing (RS). http://www.glrw.ir/fa/upload/f04641c2/306ef144.pdf
Bagherzadeh A (2012) Estimation of soil losses by USLE model using GIS at Mashhad plain, Northeast of Iran. Arab J Geosci 7(1):211–220
Bagherzadeh A, Mansouri Daneshvar M (2010) Estimating and mapping sediment production at Kardeh watershed by using GIS. The 1st International Applied Geological Congress, Department of Geology, Islamic Azad University, Mashad Branch, Iran
Barmaki M, Pazira E, Hedayat N (2011) Investigation of relationships among the environmental factors and water erosion changes using EPM model and GIS. Int Res J Appl Basic Sci 3(5):945–949
BCEOM (1998) Abay River Basin Integrated Development Master Plan, Main Report. Ministry of Water Resources, Addis Ababa
Beasley DB, Huggins LF, Monke EJ (1980) ANSWERS: a model for watershed planning. Trans ASCE 23:938–944
Behrens T, Föster H, Scholten T, Steinrücken U, Spies E, Goldschmitt M (2005) Digital soil mapping using artificial neural networks. J Plant Nutr Soil Sci 168:21–33
Biesemans J, Van Meirvenne M, Gabriels D (2000) Extending the RUSLE with the Monte Carlo error propagation technique to predict long-term average off-site sediment accumulation. J Soil Water Conserv 55:35–42
Bonilla CA, Reyes JL, Magri A (2010) Water erosion prediction using the revised universal soil loss equation (RUSLE) in a GIS framework, Central Chile. Chil J Agric Res 70(1):159–169
Bozorgzadeh E, Kaman N (2012) A geographic information system (GIS)-based modified erosion potential method (EPM) model for evaluation of sediment production. J Geol Min Res 4(6):130–141
Bryan RB (2000) The concept of soil erodibility and some problems of assessment and application. Catena 16:393–412
Cochrane TA, Flanagan DC (2003) WEPP watershed modeling with DEM's and GIS: the representative hill slope profile method. Trans Am Soc Agric Eng 46(4):1041–1049
Conacher AJ, Dalrymple JB (1977) The nine-unit land surface model: an approach to pedo-geomorphic research. Geoderma 18:1–154
Congalton RG, Green K (1999) Assessing the accuracy of remote sensing data: principle and practises. CRC Press Inc, Denvers 173p
Conoscenti C, Angileri S, Cappadonia C, Rotigliano E, Agnesi V, Märker M (2013) Gully erosion susceptibility assessment by means of GIS-based logistic regression: a case of Sicily (Italy). Geomorphology. In Press. doi:10.1016/j.geomorph.2013.08.021
Conoscenti C, Agnesi V, Angileri S, Cappadonia C, Rotigliano E, Märker M (2014) A GIS-based approach for gully erosion susceptibility modelling: a test in Sicily, Italy. Environ Earth Sci 70(3):1179–1195
Conrad O (2007) SAGA—Entwurf, Funktionsumfang und Anwendung eines Systems für Automatisierte Geowissenschaftliche Analysen. Dissertation, University of Göttingen
De Rosa P (2005) Analisi e confronti di modelli di erosione del suolo e tra-sporto di sedimenti tramite l'uso di sistemi G.I.S. Degree Thesis, Universitá degli studi di Perugia, Italia
Dehbozorgi M, Pourkermani M, Arian M, Matkan AA, Motamedi H, Hosseiniasl A (2010) Quantitative analysis of relative tectonic activity in the Sarvestan area, central Zagros, Iran. Geomorphology 121(3–4):329–341

Dikau R (1989) The application of a digital relief model to landform analysis in geomorphology. In: Raper J (ed) Three dimensional application in Geographic Information Systems. London, pp 51–77
Eisazadeh L, Amani RS, Pazira E, Homaee M, Sokouti R (2012) Comparison of empirical models to estimate soil erosion and sediment yield in micro catchments. Int J Agric Res Rev 2(3):303–307
Elith J, Leathwick JR, Hastie T (2008) A working guide to boosted regression trees. J Anim Ecol 77:802–813
Elsenbeer H, Cassel DK, Tinner W (1993) Daily rainfall erosivity model for western Amazonian. J Soil Water Conserv 48:439–444
FAO (1994) Land degradation in South Asia: its severity causes and effects upon the people. FAO, UNDP and UNEP report, Rome
Faulkner H, Alexander R, Teeuw R, Zukowskyj P (2004) Variations in soil dispersivity across a gully head displaying shallow sub-surface pipes, and the role of shallow pipes in rill initiation. Earth Surf Process Land 29:1143–1160
Feiznia S (2000) Rock resistance against corrosion in different climates in Iran. Nat Resour J 47:95–116 Iran (in Persian)
Feiznia S, Ahzan K (2004) Determining soil erodibility of Damavand basin with USLE model. Sediment Sediment Rock J 4:13–29 (in Persian)
Ferro V, Giordano G, Iovino M (1991) Isoerosivity and erosion risk map for Sicily. Hydrol Sci J 36:549–564
Flanagan DC, Nearing MA (1995) USDA water erosion prediction project: hillslope profile and watershed model documentation. NSERL Report No. 10. USDA-ARS National Soil Erosion Research Laboratory, West Lafayette
Friedman JH (1999) Stochastic gradient boosting. Technical Report. Department of Statistics, Stanford University, USA. http://www.salford-systems.com/treenet.html
Friedman JH (2002) Stochastic gradient boosting. Comput Stat Data Anal 38:367–378
Gee GW, Bauder JW (1986) Particle-size analysis. In Burt R (ed) Soil survey field and laboratory methods manual; report no 51: 53–54, US Department of Agriculture, Lincoln, Nebraska
Gobin A, Jones R, Kirkby M, Campling P, Govers G, Kosmas C, Gentile AR (2004) Indicators for pan-European assessment and monitoring of soil erosion by water. Environ Sci Policy 7(1):25–38
Grove AT, Rackham O (2001) The nature of Mediterranean Europe: an ecological history. Yale University Press, New Haven
Hoseini S, Gorbani M (2005) Economics of soil erosion. Ferdowsi University of Mashhad Press, Mashhad (in Persian)
Hosmer DW, Lemeshow S (2000) Applied logistic regression. Wiley series in Probability and Statistics
Hu Q, Clark JG, Jung P, Lee B (2000) Rainfall erosivity in the Republic of Korea. J Soil Water Conserv 55(2):115–120
Ilanloo M (2012) Estimation of soil erosion rates using MPSIAC models (Case Study Gamasiab basin). Int J Agric Crop Sci 16:1154–1158
Jianping G, Niu T, Rahimy P, Wang F, Zhao H, Zhang J (2012) Assessment of soil erosion susceptibility using empirical modeling. J Acta Meteorol Sin 27(1):98–109
Kakembo V, Xanga WW, Rowntree K (2009) Topographic thresholds in gully development on the hillslopes of communal areas in Ngqushwa Local Municipality, Eastern Cape, South Africa. Geomorphology 110(3–4):188–194
Karami A, Homaee M, Neyshabouri MR, AfzalInia S, Basirat S (2012) Large scale evaluation of single storm and short/long term erosivity index models. Turk J Agric For 36:207–216
Kefi M, Yoshino K, Setiawan Y, Zayani K, Boufaroua M (2011) Assessment of the effects of vegetation on soil erosion risk by water: a case of study of the Batta watershed in Tunisia. Environ Earth Sci 64(3):707–719
Kheir R, Wilson J, Deng Y (2007) Use of terrain variables for mapping gully erosion susceptibility in Lebanon. Earth Surf Process Land 32:1770–1782
Kirkby M (2001) Modelling the interactions between soil surface properties and water erosion. Catena 46:89–102
Kompani-Zare M, Soufi M, Hamzehzarghani H, Dehghani M (2011) The effect of some watershed, soil characteristics and morphometric factors on the relationship between the gully volume and length in Fars Province, Iran. Catena 86(3):150–159
Köthe R, Lehmeier F (1993) SARA - Ein Programmsystem zur Automatischen Relief-Analyse. Z. f. Angewandte Geographie, 4/93:11-21; Cologne, Germany
Kouli M, Soupios P, Vallianatos F (2009) Soil erosion prediction using the revised universal soil loss equation (RUSLE) in a GIS framework, Chania, Northwestern Crete, Greece. Environ Geol 57:483–497

Kumar BM, Nair PKR (2006) Tropical homegardens: a time-tested example of sustainable agroforestry. Springer Science, Dordrecht 380p
Lal R (2001) Soil degradation by erosion. Land Degrad Dev 12:519–539
Landi A, Barzegar AR, Sayadi J, Khademalrasoul A (2011) Assessment of soil loss using WEPP model and geographical information system. J Spat Hydrol 11(1):40–51
Le Roux JJ, Morgenthal TL, Malherbe J, Pretorius DJ, Sumner PD (2008) Water erosion prediction at a national scale for South Africa. Water SA 34, http://www.wrc.org.za. (last view 30.01.2015)
Leh M, Bajwa S, Chaubey I (2011) Impact of land use change on erosion risk: an integrated remote sensing, geographic information system and modeling methodology. Land Degrad Dev 24:409–421. doi:10.1002/ldr.1137
Lesschen JP, Kok K, Verburg PH, Cammeraat LH (2007) Identification of vulnerable areas for gully erosion under different scenarios of land abandonment in Southeast Spain. Catena 71:110–121
Maerker M, Angeli L, Bottai L, Costantini R, Ferrari R, Innocenti L, Siciliano G (2008) Assessment of land degradation susceptibility by scenario analysis: a case study in Southern Tuscany, Italy. Geomorphology 93:120–129
Mahmoodabadi M, Refahi HG (2005) Sediment yield assessment using MPSIAC model in GIS framework. Tehran University, Tehran
Masoudi M, Zakerinejad R (2010) Hazard assessment of desertification using MEDALUS model in Mazayjan plain, Fars province, Iran. Ecol Environ Conserv 16(3):425–430
Masoudi M, Zakerinejad R (2011) A new model for assessment of erosion using desertification model of IMDPA in Mazayjan plain, Fars province, Iran. Ecol Environ Conserv 17(3):489–594
Masoudi M, Patwardhan AM, Gore SD (2006) Risk assessment of water erosion for the Qareh Aghaj subbasin, southern Iran. Stoch Env Res Risk Assess 21:15–24
Meamarian H, Esmaeilzadeh H (2003) The Sediment yield potential estimation of Kashmar watershed (Iran) using MPSIAC model in the GIS framework. http://www.gisdevelopment.net/application/2003. (last view 30.01.2015)
Mitas L, Mitasova H (1998) Distributed soil erosion simulation for effective erosion prevention. Water Resour Res 34:505–516
Mitasova H, Mitas L (2001) Multiscale soil erosion simulations for landuse management. In: Harmon R, Doe W (eds) Landscape erosion and landscape evolution modeling. Kluwer Academic/Plenum Publishers, Dordrecht, pp 321–347
Mitasova H, Hofierka J, Zlocha M, Iverson LR (1996) Modelling topographic potential for erosion and deposition using GIS. Int J Geogr Inf Syst 10:629–641
Moore D, Wilson JP (1992) Length-slope factors for the revised universal soil loss equation: simplified method of estimation. J Soil Water Conserv 47:423–428
Morgan RPC (1995) Soil erosion and conservation. 2nd edn. Longman, London, 198 pp
Morgan RPC, Quinton JN, Smith RE, Govers G, Poesen JWA, Auerswald K, Chisci G, Torri D, Styczen ME (1998) The European Soil Erosion Model (EUROSEM): a dynamic approach for predicting sediment transport from fields and small catchments. Earth Surf Process Land 23:527–544
Moussavi E, Nikkami D, Mahdian MH, Pazir A (2012) Investigating rainfall erosivity indices in arid and semi arid climates of Iran. Turk J Agric For 36:365–378
Najm Z, Keyhani N, Rezaei K, Naeimi Nezamabad A, Vaziri H (2011) Sediment yield and soil erosion assessment by using an empirical model of MPSIAC for Afjeh & Lavarak sub-watersheds, Iran. Earth Sci J 2(1):14–22
Najmoddini N (2003) Assessment of erosion and sediment yield process using RS and GIS. M.Sc. Thesis, International institute for Geo-Information science and earth observation (ITC), the Netherlands, 63p
Nazari Samani A, Ahmadi H, Jafari M, Boggs G (2009) Geomorphic threshold conditions for gully erosion in Southwestern Iran (Boushehr-Samal watershed). Earth Sci 35:180–189
Nearing MA, Foster GR, Lane LJ, Finkner SC (1989) A process-based soil erosion model for USDA-water erosion prediction project. Trans ASAE 32(5):1587–1593
Nikeghbal M, Rafati S (2009) A GIS-based assessment of the relationships between erosion and desertification in a semi-arid climate: Zarindasht district, Fars province, national geo informatics, Tehran, Iran
Olaya V, Conrad O (2009) Geomorphometry in SAGA. In: Hengl T, Reuter HI (eds) Geomorphometry concpets, software, applications. Developments in soil science, vol 33. Elsevier, UK, pp 293–308
Omidvar K (2010) Introduction to soil conservation and watershed, 2nd edn. Yazd University Press, Yazd (in Persian)
Onori F, Bonis PD, Grauso S (2006) Soil erosion prediction at the basin scale using the revised universal soil loss equation (RUSLE) in a catchment of Sicily (Southern Italy). Environ Geol 50:1129–1140

Pacific Southwest Interagency Committee (1968) Report of the water management subcommittee on factors affecting sediment yield in the pacific southwest area and selection and evaluation of measures for reduction of erosion and sediment yield. ASCE, 98, Report No. HY12

Pelacani S, Märker M, Rodolfi G (2008) Simulation of soil erosion and deposition in a changing land use: a modelling approach to implement the support practice factor. Geomorphology 99:329–340

Planchon O, Darboux F (2001) A fast, simple and versatile algorithm to fill the depressions of digital elevation models. Catena 46:159–176

Poesen JW, Vandaele K, Van Wesemael B (1996) Contribution of gully erosion to sediment production on cultivated lands and rangelands. In: Walling DE, Webb BW (eds) Erosion and Sediment Yield: Global and Regional Perspectives (Proceedings of the Exeter Symposium, July 1996) IAHS Publication, 236: 251–266

Popp JH, Hyatt DE, Hoag D (2000) Modeling environmental condition with indices: a case study of sustainability and soil resources. Ecol Model 130(1–3):131–143

Pradhan B, Chaudhari A, Adinarayana J, Buchroithner M (2012) Soil erosion assessment and its correlation with landslide events using remote sensing data and GIS: a case study at Penang Island, Malaysia. Environ Monit Assess 184(2):715–727

Renard KG, Freimund JR (1994) Using monthly precipitation data to estimate the R-factor in the revised USLE. J Hydrol. 157:287–306, European Commission Joint Research Centre Institute for Environment and Sustainability

Renard KG, Foster G.R, Weesies GA, McCool DK, Yoder DC (1997) Prediction soil erosion by water: a guide to conservation planning with the revised universal soil loss equation. Agricultural Handbook 703. US Department of Agriculture p. 404

Roshani MR, Rangavar A, Javadi MR, Ziyaee A (2013) A new mathematical model for estimation of soil Erosion. Int Res J Appl Basic Sci 5(4):491–497

Rusco E, Montanarella L, Bosco C (2008) Soil erosion: a main threats to the soils in Europe. In: Tóth G, Montanarella L, Rusco E (eds) Threats to soil quality in Europe. No. EUR 23438 EN in EUR—scientific and technical research series. Office for official publications of the European Communities: 37–45. Google Scholar: 16771305971362909763

Sadeghi SHR, Moatamednia M, Behzadfar M (2011) Spatial and temporal variation in the rainfall erosivity factor in Iran. J Agric Sci Technol 13:451–464

Sadeghifard D, Jabari E, Ghayasian H (2004) Rainfall erosivity zonation in Iran, the first national conference on civil engineering, Sharif University of Technology, Iran. CIVILICA online journal: http://www.civilica.com/Paper-NCCE01-226_2417394703.html, 1–8. (in Persian) (last view 30.01.2015)

Safamanesh R (2004) Validation of the MPSIAC Model for sediment yield prediction in Zargeh watershed, Iran. MSc Thesis, University Putra Malaysia

Sariyildiz T, Anderson JM, Kucuk M (2005) Effects of tree species and topography on soil chemistry, litter quality, and decomposition in Northeast Turkey. Soil Biol Biochem 37(9):1695–1706

Saxton KE, Rawls WJ (2006) Soil water characteristic estimates by texture and organic matter for hydrologic solutions. Soil Sci Soc Am J 70:1569–1578

Seibert J, Stendahl J, Sorensen R (2007) Topographical influences on soil properties in boreal forests. Geoderma 141:139–148

Shahrivar A, Tehbconsung C, Jusop S, Abdul Rahim A, Soufi M (2012) Roles of SAR and EC in Gully Erosion Development (A Case Study of Kohgiloye va Boyerahmad Province, Iran). J Res Agric Sci 8(1):1–12

Shruthi RBV, Kerle N, Jetten V (2011) Object-based gully feature extraction using high spatialresolution imagery. Geomorphology 134:260–268

Sidorchuk A, Märker M, Moretti S, Rodolfi G (2003) Gully erosion modelling and landscape response in the Mbuluzi River catchment of Swaziland. Catena 50:507–525

Simms AD, Woodroffe CD, Jones BG (2003) Application of RUSLE for erosion management in a coastal catchment, southern NSW. International Congress on Modelling and Simulation 2, Social and Economic Systems for Resource Management Solutions, Townsville, Queensland, 678–683

Suriyaprasit M (2008) Digital terrain analysis and image processing for assessing erosion prone areas. PhD Thesis, International institute for geo-information science and earth observation, The Netherlands

Tagil S, Jenness J (2008) GIS-based automated landform classification and topographic, landcover and geologic attributes of landforms around the Yazoren Polje, Turkey. J Appl Sci 8:910–921

Tangestani M (2006) Comparison of EPM and PSIAC models in GIS for erosion and sediment yield assessment in a semi-arid environment: Afzar Catchment, Fars Province, Iran. J Asian Earth Sci 27:585–597

Tangestani MH, Moore F (2001) Comparison of three principal component analysis techniques to porphyry copper alteration mapping, A case study, Meiduk area, Kerman, Iran. Can J Remote Sens 27(2): 176–182

Terranova O, Antronico L, Coscarelli R, Iaquinta P (2009) Soil erosion risk scenarios in the Mediterranean environment using RUSLE and GIS: an application model for Calabria (Southern Italy). Geomorphology 112:228–245

Vaezi AR, Sadeghi SHR (2011) Evaluating the RUSLE model and developing an empirical equation for estimating soil erodibility factor in a semi-arid region. Span J Agric Res 9(3):912–923

Valentin C, Poesen J, Yong L (2005) Gully erosion: impacts, factors and control. Catena 63:132–153

Vandekerckhove L, Muys B, Poesen J, De Weerdt B, Coppé N (2001) A method for dendrochronological assessment of medium-term gully erosion rates. Catena 45:123–161

Wang G, Gertner G, Fang S, Anderson AB (2003) Mapping multiple variables for predicting soil loss by geostatistical methods with TM image sand a slope map. Photogramm Eng Remote Sens 69:889–898

Wilson JP, Gallant JC (2000) Terrain analysis: principles and applications. Wiley, New York, 520 pp

Wischmeier WH, Smith SS (1978) Predicting rainfall-erosion losses: a guide to conservation planning. Agriculture Handbook No. 537. US Department of Agriculture, Washington, DC

Wordofa G (2011) Soil erosion modeling using GIS and RUSLE on the Eurojoki watershed Finland. Bachelor's thesis, Tampere University, Finland

Yuksel A, Akay A, Reis E, Mand Gundogan R (2007) Using the WEPP model to predict sediment yield in a sample watershed in Kahramanmaras region. Int Congr River Basin Manag 2:11–22

Yuksel A, Gundogan R, Akay AE (2008) Using the remote sensing and GIS technology for erosion risk mapping of Kartalkaya dam watershed in Kahramanmaras, Turkey. Sensors 8:4851–4865

Zakerinejad R, Märker M (2014) Prediction of Gully erosion susceptibilities using detailed terrain analysis and maximum entropy modeling: a case study in the Mazayejan Plain, Southwest Iran. Geogr Fis Din Quat 37(1):67–76

Zevenbergen LW, Thorne CR (1987) Quantitative analysis of land surface topography. Earth Surf Process Landf 12(1):47–56